ELSEVIER

Biophysical Chemistry 90 (2001) 233–248

Biophysical Chemistry

www.elsevier.nl/locate/bpc

Osmotic perturbations induce differential movements in the core and periphery of proteins, membranes and micelles

C.N. Madhavarao[a], Z.E. Sauna[a], A. Srivastava[b], V. Sitaramam[a,*]

[a] *Department of Biotechnology, University of Pune, Pune-411007, India*
[b] *Chemical Physics Group, Tata Institute of Fundamental Research, Mumbai-400 005, India*

Received 26 October 2000; received in revised form 31 January 2001; accepted 9 February 2001

Abstract

Polymeric structures, namely, micelles, membranes and globular proteins share the property of two distinct regions: a hydrophobic core and a hydrophilic exterior. The dynamics of these regions of the polymeric structures were probed using selective fluorophores 1,6-diphenyl-1,3,5-hexatriene (DPH) and 1-anilinonaphthalene-8-sulfonate (ANS), respectively. Perturbation of the polymers by external osmotic pressure, ionic strength and temperature was monitored in the two regions using steady state measurements of fluorescence intensity and anisotropy. While the fluorescence lifetime of DPH and ANS did not change significantly, parallel change in steady state anisotropy values and the rotational correlation time indicated mobility in the probe/probe-domain. Osmotic perturbation of the polymers in electrolyte media led to decreased DPH mobility. Enhanced ellipticity at 222 nm in bovine serum albumin was observed in 1.5 M NaCl and sucrose media. ANS exhibited a decreased anisotropy with progressive dehydration in proteins in NaCl media, in dimyristoylphosphatidylcholine (DMPC) vesicles in sucrose media, and in neutral laurylmaltoside micelles in both NaCl and sucrose media. Thus, ANS showed responses opposite to that of DPH in these systems. A comparison with several domain selective probes indicated that DPH reported findings common to depth probes while ANS reported data common to interfacial probes used for voltage monitoring.

Keywords: Fluorescence anisotropy; BSA; DMPC vesicles; Laurylmaltoside micelles

Abbreviations: ANS, 1-anilinonaphthalene-8-sulfonate; BSA, bovine serum albumin; DPH, 1,6-diphenyl-1,3,5-hexatriene; DMPC, dimyristoylphosphatidylcholine; LM, laurylmaltoside (*n*-dodecyl-β-D-maltoside); LUV, large unilamellar vesicles; *n*-AS, *n*-(9-anthroyloxy) stearic acid; NRSS, normalised residual sum of squares; S.E.M., standard error of mean; TMRM, tetramethylrhodaminemethylester

* Corresponding author. Tel.: +91-20-565-5179; fax: +91-20-565-5179.
E-mail address: sitaram@unipune.ernet.in (V. Sitaramam).

0301-4622/01/$ - see front matter
PII: S0301-4622(01)00144-2

1. Introduction

Exposure of polymers such as proteins, membranes and micelles to external solutes at concentrations large enough to compete for water of hydration has structural consequences [1–3]. These biologically relevant polymers themselves are compact structures such that in these condensed states, the energy levels associated with elastic (including torsional, bending, etc.) as well as electrostatic interactions are nearly at the same level since both markedly affect the behaviour of these polymers [4,5]. Some of the polymers respond more to electrostatic perturbations, as with ionic strength (e.g. proteins), while others respond more to elastic changes (e.g. liposomal membranes; [6]).

Dehydration, generally (by addition of solutes, frank removal of bulk water by freeze drying, addition of organic solvents, etc.) is considered to cause compaction of the polymer and spaces within [7,8]. If the polymer is uniformly and equally interconnected, it would be either rigid (frozen) or flexible such that, on dehydration, it would be uniformly rigid everywhere. Failure to do so would indicate unanticipated interactions, possibly in specific regions. Therefore, it would be of interest to examine whether interfacial and hydrophobic fluorescence probes (which reside in such internal spaces or voids) would respond to decreased chemical potential of water in the medium in the same manner and whether compaction is the rule. Cross comparisons between different kinds of polymers could circumvent chemical specificity and would help delineate the physical interactions.

Proteins, membranes and micelles possess a hydrophobic interior and a hydrophilic exterior [9–12]. These regions could be usefully probed with relatively selective fluorescent probes, DPH for the hydrophobic interior [13] and ANS for the relatively hydrophilic interface [14] and the latter's binding is influenced by the surface charges [15,16]. The movements within these regions could be probed by fluorescence anisotropy. Electrostatic repulsion in proteins could be overcome by screening the surface charges by electrolytes, leading to enhanced (thermal) movements in the protein exterior. This increased mobility with the ionic strength could have a direct consequence on the fluorescent probe embedded in that domain leading to a decrease in fluorescence anisotropy. Such effects should be seen primarily in proteins, less so in DMPC vesicles and may well be absent in neutral detergent micelles such as laurylmaltoside. On the other hand, if other interactions dominate, such a broad-based comparison should invoke diverse responses due to different mechanisms. The results presented in this study indicate: (i) a variety of surface/interfacial probes yield changes in anisotropy, which cannot be ascribed to charge neutralisation alone; and (ii) the interior and exterior of these polymers appear to have unanticipated, reciprocal (i.e. inversely correspondent), rather than directly related, dynamics, which are measurable under osmotic perturbations.

2. Experimental procedures

2.1. Materials

Proteins, BSA and ovalbumin, DMPC, D_2O, all non-electrolytes, DPH, ANS and merocyanin 540 were purchased from Sigma, USA. The *n*-AS probes and TMRM were bought from Molecular Probes Inc., USA. Laurylmaltoside and the organic solvents were bought from Fluka, Switzerland. The analytical grade NaCl and NaH_2PO_4 were bought from Merck, India. ANS and DPH were recrystallised in ethanol before use, while other chemicals and proteins were used without further purification. Reagent-grade water (Labconco, USA) was used throughout the experimentation.

2.2. Precautions in fluorescence experiments

The high solute concentrations used in the present studies precluded routine binding studies due to high viscosities/densities. Interferences would be more, not normally encountered in the usual biochemical experiments with dilute solutions. In order to circumvent the interferences the experiments were done with the following

precautions. (i) The macromolecules/polymer assemblies were pre-incubated with the dye before they were exposed to various solutes. (ii) All organic solvents were freshly distilled. (iii) The scatter contribution, if any, from the solutions of all concentrations were systematically deducted. (iv) No two dyes were used together since the interferences for any reason including energy transfer could be a variable. (v) Intrinsic tryptophan fluorescence was measured only in the absence of any external dye. (vi) Detailed experiments were done with each of the solutes for interferences. (vii) Sugars, particularly the aged samples, contributed heavily to signals as well as background scatter and all such bottles were routinely screened and eliminated due to obvious contamination. (viii) Conductance (to eliminate salt contamination), surface tension (to eliminate detergent contamination) and UV-vis spectra of the highly concentrated solutions were routinely recorded on all solutes before accepting them for experiments.

2.3. Fluorescence measurements in proteins

Fluorescent dyes, ANS and DPH were added to the protein at final concentrations of 25 μM and 12.5 μM, respectively. A stock solution of ANS was made in distilled water and that of DPH in tetrahydrofuran. Additions were made such that the final concentration of tetrahydrofuran did not exceed 0.25%. Solutions for measurements consisted of 250 μg/ml of protein, 10 mM sodium phosphate buffer, pH 7.4 and either 12.5 μM DPH or 25 μM ANS. Protein was incubated with ANS or DPH in the dark for 30 min prior to measurements. Excitation and emission wavelengths for the probes were: ANS, excitation 350 nm and emission 470 nm; DPH, excitation 355 nm and emission 440 nm.

Fluorescence measurements were carried out at a specific temperature, 25 ± 0.5°C, using a Kontron SFM 25 spectrofluorometer with continuous stirring. Fluorescence anisotropy was calculated from fluorescence polarisation, P, [13] as

$$P = (I_{vv} - GI_{vh})/(I_{vv} + GI_{vh}) \quad (1)$$

where G is given by (I_{hh}/I_{hv}) and anisotropy, $r = (2P)/(3 - P)$. I is the fluorescence intensity, v and h stand for the polariser placed vertically and horizontally, respectively, and the double subscripts stand for the excitation and emission polarisers, respectively. The correction factor 'G' was calculated at every polarisation value using the horizontally polarised light (i.e. for each polarisation value, a set of four fluorescence measurements were used with the excitation and emission polarisers oriented in all four combinations). In all measurements reported here, the G value was seen to be close to 1.0 (range 1.0–1.25) thereby ensuring that the emission monochromator did not contribute significantly to polarisation effects at the wavelengths used. The spectrofluorometer was interfaced via the RS232 C port to a 286 IBM compatible computer and polarisation measurements were made in the automated mode. For each reading, 25 polarisation measurements were made at 12-s intervals, and averaged. Steady state anisotropy values above 0.1 were reproducible within 5% for most probes day-to-day. Low anisotropy values ($\ll 0.1$) varied at most by 30%. However, the trends were highly comparable in all the experiments reported. Comparisons were made between different treatments with the same samples on the same day. The polarisation and fluorescence intensity measurements were made using only polarisation module to ensure comparable conditions of measurement.

2.4. Fluorescence measurements in micelles

A stock solution of laurylmaltoside was made in 10 mM Tris–HCl, pH 7.4. Aliquots of the stock were suspended in various NaCl and sucrose concentrations such that the final concentration was 5 mg/ml, i.e. almost nine times the critical micellar concentration. The respective fluorescent probes were added and incubated in the dark for 15 min before measurements. ANS was added to a final concentration of 25 μM and DPH for 12.5 μM. Stock solutions of merocyanin-540, TMRM and n-AS probes were made in ethanol and added to a final concentration of 10, 5 and 10 μM, respectively. The excitation and emission wavelengths for ANS were 350 nm and 470 nm; for

DPH, 355 nm and 430 nm; for merocyanin-540, 555 nm and 580 nm; for TMRM, 520 nm and 574 nm and for *n*-AS probes, 360 nm and 440 nm, respectively. Fluorescence intensity and anisotropy measurements were made at 25 ± 0.5°C as described for proteins.

Temperature scans were done with a continuous temperature ramp of 0.5°C/ min, using a Haake waterbath and Haake F3 thermoregulator controlled by a PG 20 programmer (Haake). The actual temperature in the cuvette was independently monitored using a temperature probe connected to a Hewlett-Packard 89100A temperature controller and recorded on a Hewlett-Packard 85B microprocessor. Continuous on-line measurements of fluorescence anisotropy and fluorescence intensity were made on a Kontron SFM 25 spectrofluorometer and accumulated every 12 s onto an IBM compatible PC.

2.5. Fluorescence measurements in membranes

LUVs, having a mean diameter of approximately 100 nm were prepared by reverse phase evaporation as described in Szoka and Papahadjopoulos [17]. Vesicles contained 10 mM sodium phosphate buffer pH 7.4, 200 mM sucrose and 10 mM NaCl. Vesicles were pre-incubated with the fluorescent probes (ANS or DPH) for 30 min in the dark. Final concentrations of ANS and DPH were 25 μM and 12.5 μM, respectively. Aliquots of LUVs, equivalent to 500 μg/ml of lipid, were used for osmotic titrations with NaCl and sucrose in 10 mM sodium phosphate buffer, pH 7.4. Fluorescence intensity and anisotropy measurements were made at 30 ± 0.5°C as described for proteins.

2.6. Binding studies

DPH and ANS binding to BSA were carried out as described in Rubalcava et al. [18], using the Klotz equation given below.

$$(P_o/xD_o) = (1/n)\left[1 + \left\{K_{app}/(1-x)D_o\right\}\right] \qquad (2)$$

where P_o and D_o are the total protein and dye concentrations, respectively; x is the fraction of the dye bound (which is obtained from the quotient of the fluorescence intensity (q) to that derived from a plot of fluorescence intensity vs. varying dye concentration at a fixed protein concentration). The quantum yield (q) or the total fluorescence intensity was obtained as F_{max} (i.e. when all the dye molecules were bound, at fixed dye concentration) in a direct linear plot [19] of fluorescence vs. varying protein concentration. The number of binding sites '*n*' was (expressed as the mol of dye bound per mol of protein) obtained as the hyperbolic asymptote from a plot of $[(1-x)D_o]$ vs. (xD_o/P_o). The direct linear plot was preferred to estimate parameters of the hyperbolic relationships as the method yields robust estimates of the parameters and does not face the problem of non-convergence that non-linear iterative methods are prone to. The reliability of the fits for the non-linear relationship was assessed in terms of the residual sum of squares, normalised for the total variance of the *y*-variable, to obtain a scale-free measure of error (NRSS), which simply reduces to $(1-r^2)$ in the case of linear regression.

2.7. Fluorescence lifetime measurements

2.7.1. Time-domain measurements

Fluorescence lifetime of DPH was measured using the 358-nm pulse (FWHM ~ 1.2 ns) from a nitrogen flash lamp (IBH Consultants, UK). A 420-nm cut-off filter was used on the emission side. An epifluorescence microscope (Nikon Diaphot 300) with a dichoric mirror at 400 nm was used in these experiments. Time-correlated single-photon-counting set-up was used in the measurement of fluorescence lifetimes.

Fluorescence decay curves of the intrinsic tryptophan and ANS were analysed by deconvoluting the decay curves with the instrument response function (IRF), to obtain the fluorescence intensity decay function as,

$$I(t) = \sum \alpha_i \exp(-t/\tau_i) \qquad (i = 2 \text{ or } 3) \qquad (3)$$

and the average lifetime was computed as,

$$\tau_{avg} = \Sigma\alpha_i\tau_i \quad (4)$$

where $I(t)$ is the fluorescence intensity, τ_i is the fluorescence lifetime and α_i is the fractional amplitudes of the fluorescence lifetimes such that $\Sigma\alpha_i = 1.0$. Non-linear least squares and Marquardt algorithm was used to extract α_i and τ_i using the iterative reconvolution method [20]. Criterion for best fit was the least χ^2 given as,

$$\chi^2 = \Sigma_i^n\left[\left((C_f - C)^2(1/n)\right)/C_f\right] \quad (5)$$

where, C_f is the counts fitted, C is the experimental counts and n is the number of channels contributing data in the determination of the lifetime components. In the absence of any systematic noise χ^2 values tend to be very close to 1.0 [21].

Perrin's equation describes the general relation between fluorescence depolarisation of a fluorescent molecule and the hydrodynamic properties of the surrounding environment. A general form of the Perrin equation assumes that [13]:

$$r_o/r = 1 + (\tau/\phi) \quad (6)$$

where, r_o is the limiting anisotropy when the probe is completely immobilised (0.362 for DPH), r, the steady state anisotropy, τ is the fluorescence lifetime of the probe in the medium and ϕ is the rotational correlation time. Variations in r would imply variations in ϕ, the probe mobility, only and if only coincident changes in τ are accounted for [22].

2.7.2. Frequency domain measurements

Fluorescence lifetimes of exogenous probes in BSA and LM micelles in 10 mM sodium phosphate buffer and buffered saline solutions were determined by measuring phase angles (θ) and modulation factors (m) in a multi-frequency phase-modulation spectrofluorometer, Fluorolog Tau-3 (ISA Jobin Yvon, New Jersey, USA). The spectrofluorometer was completely interfaced to a computer, which in turn was run by proprietary software installed on another computer with a pentium III processor. The light source was a 450-W xenon lamp and excitation wavelength was chosen through a double grating monochromator. Sinusoidal modulation of light was achieved by a Pockels cell. The spectrofluorometer was standardised to yield a lifetime with a single exponential decay of 1.35 ns for POPOP (*p*-bis[2-(5-phenyloxazolyl)]benzene) in methanol. The frequencies were chosen between 5 and 225 MHz. Emission was collected using cut-off filters (Schott, FWHM of 10 nm for 75% transmission) in the T-channel. Emission cut-off filters were chosen such that a minimum of 40% transmission was allowed at the emission peak wavelength and 0% transmission was allowed at a minimum of 20 nm above the excitation wavelength. Signals were collected taking the polarisers out of the light path for lifetime measurement. Anisotropy decay measurement of TMRM was made in T-mode with polarisers in light path. The reference cell contained glycogen in all the lifetime measurements. Seven discrete pairs of measurements were made in all cases of sample and reference with a minimum of 6 s integration time for every measurement, at each frequency, for good χ^2 statistics based on the experience with POPOP measurements. The apparent lifetimes, τ_θ and τ_m, are related to the phase angle and modulation factors thus [22],

$$\tau_\theta = \tan\theta/\omega \quad (7)$$

$$\tau_m = (1/\omega)[(1/m^2) - 1]^{0.5} \quad (8)$$

where, ω is the circular frequency such that $\omega = 2\pi$ Hz.

Data were subjected to analyses assuming a heterogeneous decay with 2–3 lifetime components. The phase angle and modulation data were analysed by both non-global analysis and by global analysis. The software (MS Windows 98 version) developed by M.L. Johnson at the Center for Fluorescence Spectroscopy, University of Maryland School of Medicine, Baltimore, USA (http://cfs.umbi.umd.edu/cfs/software/) was used, which makes use of Nelder-Mead Simplex algorithm for parameter estimation. Lifetime

components were defined as global and their fractional contributions were allowed to change to determine if they change significantly. The confidence intervals were obtained by performing 10 000 Monte Carlo iterations. The goodness of fit was given as the value χ^2_R,

$$\chi^2_R = (1/\nu)\Sigma\left[(\theta_i - \theta_{ci})/\sigma_i^{\theta}\right]^2 + (1/\nu) \times \Sigma[(m_i - m_{ci})/\sigma_i^{m}]^2 \quad (9)$$

where the subscript i stands for the ith frequency and c stands for the computed value. The experimental error was represented as σ, superscripts correspond to phase angle and modulation, respectively, and ν is the degrees of freedom such that $\nu = 2n\lambda - p$, where, n is the number of frequencies used in the data, λ is the number of wavelengths and p is the number of parameters estimated.

2.8. CD spectra of BSA

Circular dichroism spectra were recorded on a JASCO-J715 spectropolarimeter and analysed using the software J-700 for windows, version 1-50-01 (JASCO, Inc., Easton, MD, USA). Bovine serum albumin CD spectra were recorded in the presence of 10 mM sodium phosphate buffer (pH 7.4), with various solutes after incubation for 10 min at room temperature. A 1.0-cm path length cuvette was used and the protein concentration was kept constant at 23 μg/ml. Corresponding blanks (without protein) were recorded and subtracted from the sample spectra. All spectra analysed were the average of six recordings. The stability of the ellipticity signal was independently determined using an 18-mer single stranded DNA at 25 μg/ml, in solution containing 100 mM NaCl and 10 mM sodium borate, pH 9.0. The standard deviation for the six recordings was 0.1–0.2 mdeg in the range of 200–300 nm, and ensured a signal to noise ratio of >200 in the range of 208–230 nm.

3. Results and discussion

3.1. Changes in proteins as a function of ionic strength

DPH binding to BSA was feasible to determine with fluorescence, since it did not yield a measurable fluorescence signal in aqueous solutions. Scatchard analysis according to the method of Klotz [18] showed that ~ 1.8 mol of DPH would bind with 1.0 mol of BSA. The fluorescence was first order with regard to the protein used. The probe was used at a concentration approximately four times the K_a (dissociation constant) which corresponded to attenuated response of fluorescence to probe concentration. Binding studies indicated that the K_a value was of the order of 3 μM for binding of DPH. Dialysis over three changes in 24 h with 50 volumes of the medium led to retention of more than 85% of the DPH fluorescence intensity, indicating a relatively strong intercalation inside BSA. Whereas ANS has a number of binding sites on BSA, some are relatively strong (approx. 5) and many are weak (~ 90), the binding sites were determined to be large [15,23,24]. ANS response, therefore, would be predominantly a global response of the surface/interface of the polymer.

BSA and ovalbumin are reported to be proteins with the highest intrinsic compressibility [25] and therefore would be ideal for studies on intramolecular movements. Fig. 1 shows that as the concentration of external NaCl increased, the anisotropy of DPH progressively increased in BSA (Fig. 1a) and ovalbumin (Fig. 1c) indicating compaction of the polymers. The intrinsic Trp anisotropy changes in BSA were comparable to that of DPH (Fig. 1b). A direct correlation ($r = 0.83$; $P < 0.01$) was observed between these two hydrophobic probes, Trp and DPH, for their anisotropy values in BSA (inset to Fig. 1b). The fluorescence anisotropy of ANS on the other hand decreased in these proteins. In proteins which are markedly influenced by electrostatic interactions (BSA has 198 charged residues with a net negative charge of 17 at pH 7.4; cf. [26]), enhanced

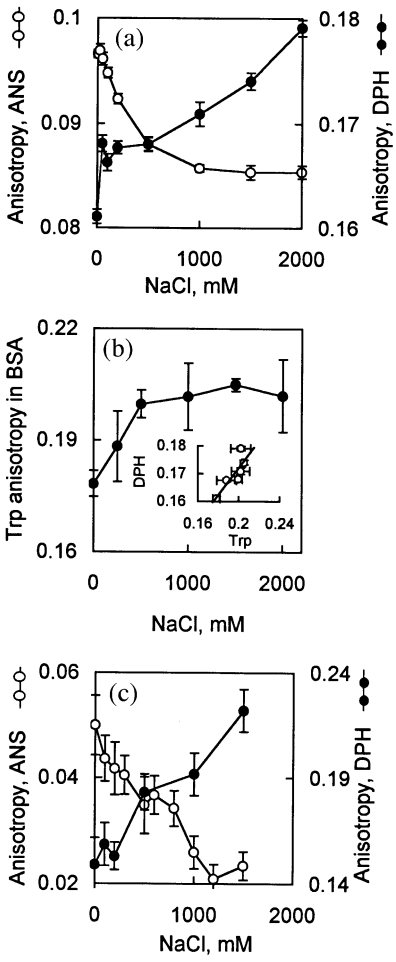

Fig. 1. Fluorescence anisotropy of ANS, DPH and Trp in BSA and ovalbumin with increasing NaCl concentration. Anisotropy changes of ANS and DPH in BSA as a function of NaCl concentration (a). Intrinsic Trp anisotropy changes in BSA as a function of NaCl concentration (b). Inset shows the direct correlation ($r = 0.83$; $P < 0.01$) between the observed anisotropy values of Trp (x-axis) and DPH (y-axis) in BSA. Anisotropy changes of ANS and DPH in ovalbumin as a function of NaCl concentration (c). Protein ~ 250 μg/ml was incubated in the dark in NaCl solutions containing 10 mM sodium phosphate buffer, pH 7.4, after addition and mixing of either 25 μM ANS or 12.5 μM DPH, for 30 min. All the measurements were done at 25 ± 0.5°C. Data points are mean ± S.E.M. of 25 readings.

loop mobility due to screening of charges in electrolyte media [4,5] could impart enhanced mobility to ANS.

CD spectra of BSA (Fig. 2) in varying concentrations of NaCl and sucrose showed enhanced ellipticity characteristically at 222 nm (buffer, −35.02; 1.5 M NaCl, −38.06; 1.5 M sucrose, −39.28 mdeg). When plotted on an osmolality scale (Fig. 2, inset, a), the ellipticity at 222 nm showed a singular curvi-linear relationship with increasing osmolality, irrespective of whether the external solute was NaCl (−37.84, −38.49, −39.28 mdeg, at 640, 1555, 2730 mOs/kg, respectively) or sucrose (−35.02, −37.76, −38.06 mdeg, at 33 (buffer only), 963, 2873 mOs/kg, respectively). These solutes were not denaturing even at the high concentrations used (Fig. 2), while 8 M urea was denaturing (Fig. 2, inset, b) as evidenced by CD spectra. The ellipticity signal in BSA as a function of increased osmolality was consistent with increased helical content or helix rigidity. This was also argued to be due to increased stabilisation of secondary structure, as a result of compaction (better packing) or increased hydrophobicity of α-helices (cf. [27,28]).

It should be noted that fluorescence intensity of DPH and ANS in these proteins invariably showed an increase over a finite range of solute concentration consistent with plausible dehydration effect due to decreased chemical potential of water (data omitted). At higher concentrations, secondary effects supervened.

3.2. Anisotropy changes in membrane vesicles as a function of osmolarity

DMPC carries one negative charge and one positive charge due to phosphate and choline, respectively, and the net charge remains zero, unlike BSA or other proteins whose net charge depends on the total charged residues in the polypeptide, pH of the medium and the ionic strength of the medium. Therefore, DMPC vesicles were investigated for changes in anisotropy of DPH and ANS as a function of electrolyte (NaCl) and non-electrolyte (sucrose) solute concentrations. The possible confounding influence of the physical state of the vesicles was minimised by restricting the temperature to above (i.e. 30 ± 0.5°C) the phase transition temperature of DMPC (~ 24°C) for all measurements. Molecular move-

ments would also be more facilitated in the less ordered molten phase. LUVs of DMPC were chosen for the following reasons. (i) Large size admits less elastic constraints on the vesicle; and (ii) uniform single lipid ensures unambiguous interpretability. Fluorescence intensity of ANS did not show large changes in sucrose and NaCl media while DPH showed a large decrease in both (Fig. 3a,b). Surprisingly, NaCl media did not effect significant changes in the anisotropy of either DPH or ANS (Fig. 3d). On the other hand, in sucrose media, DPH anisotropy showed a progressive increase while ANS showed a decrease beyond 0.5 M sucrose (Fig. 3c). The observed decrease in ANS anisotropy was suggestive of greater mobility of the probe at the interface. DMPC vesicles possess a uniformly ordered positive and negative charge along the wall of the vesicle with zero net charge, whose influence would be further diminished by the presence of ions due to buffer. On the other hand, a protein

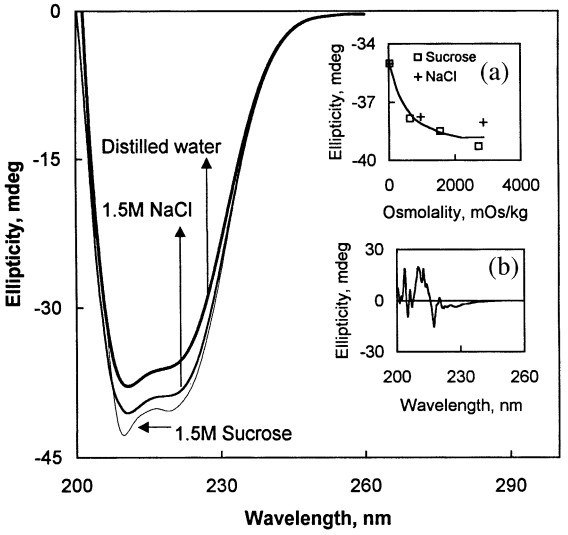

Fig. 2. Circular dichroism spectra of BSA. CD spectra were recorded in distilled water, 1.5 M NaCl and 1.5 M sucrose, all containing 10 mM sodium phosphate buffer pH 7.4 with 23 μg/ml protein. The spectra represent the average of six scans each. Inset (a) shows the ellipticity at 222 nm from the spectral data in various concentrations of NaCl and sucrose. Inset (b) is the CD spectrum of BSA denatured with 8 M urea. The data in 8 M urea was noisy at less than 215 nm owing to high tension of the photomultiplier tube.

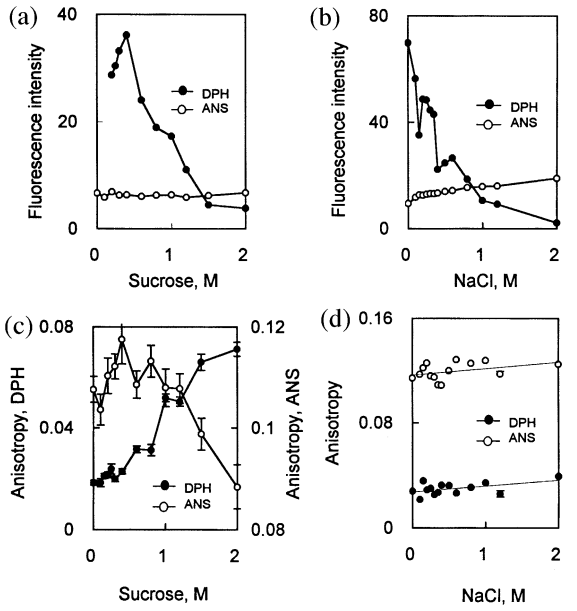

Fig. 3. Effect of sucrose and NaCl on the fluorescence intensity and anisotropy of ANS and DPH in DMPC LUVs. Fluorescence intensity changes of ANS and DPH in varying concentrations of external sucrose (a) and NaCl (b), and anisotropy changes in sucrose (c) and NaCl (d) are depicted. Measurements were made at 30 ± 0.5°C, i.e. DMPC was in the sol state. All solutions contained 10 mM sodium phosphate buffer, pH 7.4. Data points are mean ± S.E.M of 25 readings.

like BSA may show far wider complexity in the disposition of its electrostatic field. Therefore, the contribution of surface charges to this class of phenomena remained ambiguous unless one deliberately chose a neutral polymer.

3.3. Anisotropy changes in LM micelles as a function of osmolarity

The relative role of osmolarity/altered chemical potential of water vs. the role of surface charges can be resolved only by using a completely neutral (as opposed to 'net' neutral) polymer. Therefore, the micelles of a neutral detergent LM were investigated, for the effect of ionic and non-ionic osmolytes, on the responses of ANS and DPH on one hand and other interfacial probes, cationic TMRM and neutral merocyanin 540 on the other. The results were unambiguous

(Fig. 4). DPH and ANS exhibited opposing responses irrespective of whether the external osmolyte was ionic or a non-electrolyte (Fig. 4a,b, upper panels), though the magnitude was larger in sucrose media. The net charge on the fluorescent probe did not abolish the ANS-like response in that the cationic TMRM and neutral merocyanin 540 also showed a decreasing anisotropy with increasing external solute concentration (Fig. 4a,b, lower panels). Thus, ANS fluorescence anisotropy could have little to do with surface charges on the polymer or the charge on the probe per se. (i) The reason for a decrease in ANS anisotropy could be plausibly surface dehydration in these osmotic experiments, consequent of lowering the chemical potential of water at the interface due to high solute concentration. (ii) ANS exhibited a monotonic increase in fluorescence intensity (data not shown) and a blue shift in emission spectra in 2 M sucrose medium (Fig. 4c) while DPH fluorescence response was biphasic with initial increase followed by a decrease with solute concentration (data not shown). (iii) All potential sensing probes (though such probes are primarily used for changes in fluorescence intensity rather than anisotropy; cf. [29]) exhibited a response similar to ANS. (It appeared prudent to consider only such probes by pilot measurements of anisotropy, which were not excessively rigid at the interface and hence the exclusion of dyes such as oxonol-V that exhibited a very large anisotropy that was invariant with solute concentration).

The chemical potential of water in the medium may be decreased either by an increase in concentration of the same solute (which would also involve a change in the osmotic pressure) or, interestingly, by choosing solutes of increasing molecular mass at a specific concentration [2], which could be simply be due to larger solutes sequestering more water [1,2], if the relationship is monotonic, among other reasons. Differential access of the solute to the interior of the polymer is one such alternative reason. Data in Fig. 5 show that the anisotropy of both ANS and DPH

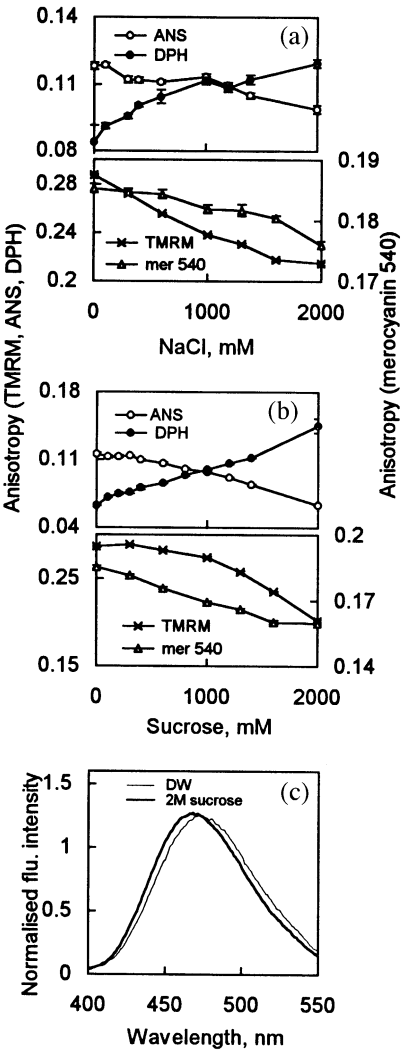

Fig. 4. Effect of NaCl and sucrose on the fluorescence anisotropy and intensity of extrinsic fluorophores in LM micelles. Anisotropy changes in media with increasing concentrations of NaCl (a) and sucrose (b) of ANS and DPH (upper panel of a and b) and other interfacial probes, TMRM and merocyanin 540 (lower panel of a and b). Emission spectra of ANS in LM micelles in 2 M sucrose medium and 10 mM Tris–HCl buffer, pH 7.4 (c). Solutions were buffered with 10 mM Tris–HCl, pH 7.4. LM was used at 5 mg/ml. The probes ANS and DPH were used at a final concentration of 25 μM and 12.5 μM, respectively. TMRM and merocyanin 540 were used at a final concentration of 5 μM and 10 μM, respectively. All measurements were done at 25 ± 0.5°C. Data points are mean ± S.E.M of 25 readings.

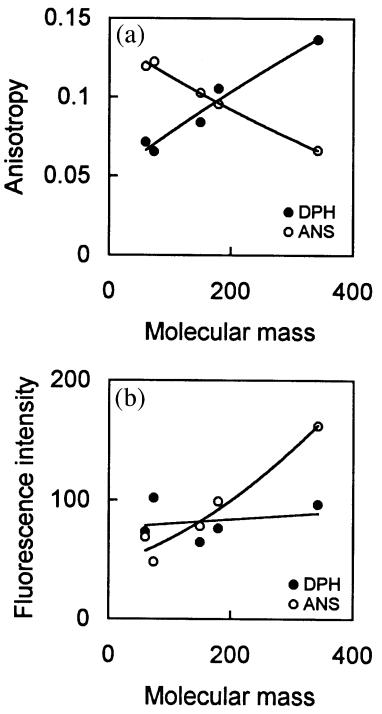

Fig. 5. Effect of increasing molecular mass of the solute on the fluorescence intensity and anisotropy of ANS and DPH in LM micelles. The solutes used were urea (60.06 Da), methylurea (74.08 Da), arabinose (150.13 Da), glucose (180.2 Da) and trehalose (342.3 Da) at 1.0 M concentration. The values in the parentheses are the molecular mass of the anhydrous solutes. Assay solutions contained 10 mM Tris–HCl, pH 7.4 and 5 mg/ml LM. Final concentrations of ANS and DPH were 25 μM and 12.5 μM, respectively. Measurements were done at 25 ± 0.5°C. Data points are mean ± S.E.M. of 25 readings (error bars are not seen due to smaller S.E.M. values).

exhibited a monotonic reciprocal relationship in the presence of osmolytes of varying molecular mass (Fig. 5a). While fluorescence intensity of ANS showed a monotonic response, DPH fluorescence was hardly molecular mass dependent at 1.0 M solute (Fig. 5b)! In other words, whatever be the basis of the molecular mass dependence, the two domains, hydrophobic interior and the hydrophilic exterior, exhibited opposite responses in terms of the dynamics of their respective domains.

3.4. Effect of temperature and deuterium oxide on the response of ANS, DPH and n-AS depth probes in LM micelles

Detailed temperature scans (Fig. 6) of the fluorescence intensity and anisotropy of DPH and ANS in these micelles helped make the following observations. (i) Presence of high sucrose in the medium consistently increased the fluorescence yield at all temperatures for both the probes. (ii) Evidence for a melting like response was marginal, if any. (iii) The anisotropy and fluorescence intensity of ANS, but not DPH, moved in different directions with temperature. (iv) Fluorescence intensity of ANS was distinctly higher in high sucrose media at lower temperatures, converged towards the level of intensity at low sucrose media as temperature increased (Fig. 6b). The difference in anisotropy in the absence and presence of high sucrose was conserved at all temperatures for both the probes (Fig. 6c,d). (v) The solutes decreased the anisotropy of ANS (Fig. 4 and Fig. 5), while temperature increased it (Fig. 6d). An important aspect was that fluorescence intensity decreased with increasing temperature as expected of enhanced access to water. However, a coincident increase in anisotropy could mean that this enhanced access to water decreased the mobility of ANS at the interface. This requires further explanation. It should be noted that DPH per se exhibited no anomalies except that its anisotropy responses were reciprocal to that of ANS thus far. The effect of temperature on DPH anisotropy and fluorescence intensity was a progressive decrease as expected of increased mobility and hydration due to higher temperatures (Fig. 6a,c). This was consistent with the published work [12,30]. The opposite response of ANS i.e. increasing anisotropy with temperature was unanticipated and hence, anomalous.

Thus, if water plays an important role in the effects seen with solutes and temperature, replacement of this water with deuterium oxide should also reflect changes consistent with dehydration. Temperature scans of fluorescence intensity and anisotropy were carried out in water and

D_2O (replacing water to the extent of 97–98%). The interfacial ANS showed a maximal effect of the presence of D_2O with increased fluorescence intensity, while DPH did not show much change (data not shown). Thus, while D_2O enhanced fluorescence yield of both the probes at all temperatures, it did so maximally at the interface suggesting that dehydration maximally affected the interface. The presence of D_2O also increased anisotropy of ANS and DPH, though marginally. These effects of temperature, solutes and D_2O were additive and not interactive.

The anomalous response of ANS in micelles was strongly linked to removal of water near the head groups of the detergent molecules and the effect of DPH was primarily opposite to that of ANS (Fig. 6). The establishment of this generality would require that any depth probe should behave similar to DPH. Experiments on fluorescence yield and anisotropy were performed incorporating the *n*-AS ($n = 2,6,9$ and 12) probes into LM micelles. The data indicated that these depth probes behaved similar to DPH (data not shown), with the added information that as depth increased, the fluorescence intensity increased as expected of hydrophobic effect and anisotropy decreased as expected of decreased order parameter in the interior [31,32].

3.5. Fluorescence lifetime values and implications for steady state anisotropy

Fluorescence lifetime data were subjected to both global and individual analyses and found to reveal negligible changes in the components of lifetime and their amplitudes. Table 1 shows the fluorescence lifetime of DPH in BSA, DMPC vesicles and LM micelles in buffer and solute media and shows that the changes in the steady state anisotropy of DPH relate to changes in rotational correlation time, ϕ, of the probe. The ϕ values, computed from the average lifetime values and steady state anisotropy [33,34] are reasonable indicators of probe mobility in its milieu [22] in the absence of anisotropy decay measurements. Table 2 and Fig. 7 show the fluores-

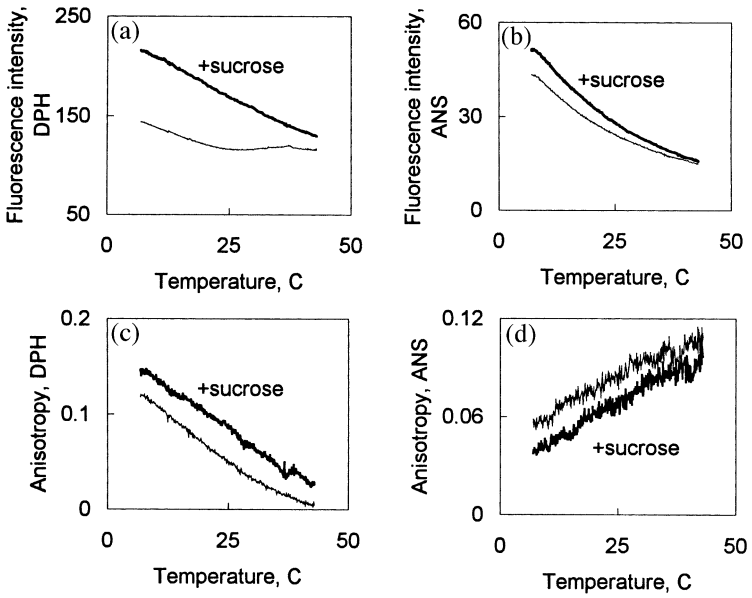

Fig. 6. Fluorescence intensity and anisotropy responses of DPH and ANS in LM micelles as a function of temperature (°C). Fluorescence intensity of DPH (a) and ANS (b) in the absence (lighter line) and presence (heavy line) of 1 M sucrose. Similarly, the anisotropy of DPH and ANS are shown in c and d, respectively. Assay solutions consisted of 10 mM Tris–HCl buffer, pH 7.4 and 5 mg/ml LM and probes ANS (25 μM) or DPH (12.5 μM). Temperature scans were performed as described under Section 2.

Table 1
Fluorescence lifetime components (τ), amplitude (α), average lifetime (τ_{avg}) and the rotational correlation time (ϕ) from the Perrin equation for DPH in BSA, DMPC LUV and LM micelles[a]

Solute, M	τ_1 (ns)	α_1	τ_2 (ns)	τ_{avg} (ns)	r	ϕ (ns)
DPH in BSA at 25 ± 0.5°C						
Control	4.05 ± 0.06	0.76 ± 0.01	9.60 ± 0.25	5.38 ± 0.07	0.162 ± 0.001	4.36 ± 0.05
1 M sucrose	3.39 ± 0.10	0.65 ± 0.02	8.07 ± 0.01	5.01 ± 0.06	0.100 ± 0.001	1.91 ± 0.02
1 M NaCl	3.32 ± 0.08	0.68 ± 0.01	8.16 ± 0.11	4.88 ± 0.06	0.173 ± 0.001	4.47 ± 0.05
DPH in DMPC LUV at 20 ± 0.5°C						
Control	5.55 ± 0.13	0.35 ± 0.07	10.94 ± 1.10	9.07 ± 0.62	ND[b]	ND
1 M sucrose	5.62 ± 0.62	0.50 ± 0.08	10.37 ± 0.33	7.98 ± 0.31	ND	ND
1 M NaCl	5.44 ± 0.17	0.40 ± 0.03	9.66 ± 0.11	7.97 ± 0.08	ND	ND
DPH in DMPC LUV at 30 ± 0.5°C						
Control	4.52 ± 0.32	0.41 ± 0.06	9.39 ± 0.18	7.38 ± 0.15	0.020 ± 0.001	0.43 ± 0.02
1 M sucrose	5.97 ± 0.48	0.69 ± 0.08	10.60 ± 0.29	7.42 ± 0.30	0.050 ± 0.002	1.19 ± 0.05
1 M NaCl	4.41 ± 0.39	0.37 ± 0.05	9.38 ± 0.21	7.55 ± 0.17	0.034 ± 0.003	0.79 ± 0.06
DPH in LM micelles at 25 ± 0.5°C						
Control	4.34 ± 0.15	0.45 ± 0.03	9.73 ± 0.14	7.28 ± 0.01	0.063 ± 0.001	1.53 ± 0.03
1.5 M NaCl	3.79 ± 0.22	0.32 ± 0.02	9.32 ± 0.11	7.57 ± 0.14	0.112 ± 0.002	2.94 ± 0.08
1 M sucrose	4.47 ± 0.17	0.46 ± 0.02	9.30 ± 0.10	7.07 ± 0.05	0.100 ± 0.001	2.70 ± 0.03
2 M sucrose	4.15 ± 0.08	0.38 ± 0.01	8.80 ± 0.05	7.03 ± 0.01	0.146 ± 0.001	4.76 ± 0.04

[a]All measurements were made in time-domain except for micelles in 1.5 M NaCl which was made in frequency domain. The values are means ± S.D.s rounded off to two decimals of a set of three measurements. τ_{avg} (average lifetime) = $\Sigma\alpha_i\tau_i$, such that $\Sigma\alpha_i = 1$. Values under column ϕ are mean ± S.D. computed of nine combinations of τ_{avg} and 'r', rounded off to two decimals. Values of 'r' represent mean ± S.E.M. of 25 readings. χ^2 values varied between 1.12 and 4.08).
[b]ND, not done.

Table 2
Components of fluorescence lifetime for ANS in BSA and LM micelles from frequency domain measurements[a]

Solute, M	τ_1 (ns)	τ_2 (ns)	τ_3 (ns)	α_1	α_2	τ_{avg} (ns)	ϕ (ns)
ANS in BSA at 25 ± 0.5°C							
Control	1.45 ± 0.14	10.18 ± 0.45	19.62 ± 0.35	0.21 ± 0.01	0.38 ± 0.02	12.18 ± 0.45	3.85 ± 0.24
1.5 M NaCl	1.45 ± 0.04	10.18 ± 0.43	17.77 ± 0.44	0.22 ± 0.01	0.44 ± 0.02	11.40 ± 0.41	3.08 ± 0.15
ANS in LM micelles at 25 ± 0.5°C							
Control	1.93 ± 0.13	6.37 ± 0.05		0.68 ± 0.01		4.94 ± 0.05	2.12 ± 0.05
1.5 M NaCl	1.93 ± 0.05	6.37 ± 0.04		0.73 ± 0.01		5.17 ± 0.05	1.72 ± 0.02
TMRM in LM micelles at 25 ± 0.5°C[b]							
Control	2.19 ± 0.07	6.30 ± 1.29		0.97 ± 0.03		2.31 ± 0.12	6.09 ± 0.28
1.5 M NaCl	2.19 ± 0.04	6.30 ± 0.13		0.95 ± 0.04		2.37 ± 0.10	2.89 ± 0.11

[a]The values are means ± S.D.s rounded off to two decimals, obtained by 10000 Monte Carlo iterations. τ_{avg} (average lifetime) = $\Sigma\alpha_i\tau_i$, such that $\Sigma\alpha_i = 1$. Values under column ϕ are mean ± S.D.s computed of nine combinations of τ_{avg} and 'r', rounded off to two decimals. χ^2_R values varied between 0.60 and 3.50.
[b]Independent measurement of anisotropy decay of TMRM in LM micelles gave single rotational correlation time of 6.58 ns and 2.33 ns in 10 mM Tris–HCl buffer, pH 7.4 and buffered 1.5 M NaCl solution, with χ^2_R values of 0.38 and 0.70, respectively, for the fits.

cence lifetime of ANS and TMRM from the frequency domain measurements. Table 2 shows three lifetimes for ANS in BSA. The average lifetime decreased in 1.5 M NaCl as compared to buffer. The longest lifetime of 19.6 ns decreased to 17.8 ns with their respective amplitudes changing in the same direction. Whereas, the lifetime of 10.2 ns did not change in NaCl as compared to buffer while its amplitude increased in NaCl, presumably, less ANS molecules reported microenvironment of lifetime of 19.62 ns and relatively more ANS molecules that of 10.2 ns. This could be a plausible situation since steady-state anisotropy also decreased with high salt in the medium (cf. Fig. 1). Data of LM micelles could also be interpreted on similar lines. Even though there is a case for role of salt in the medium on a protein, it becomes inadequate to explain similar effect observed in non-ionic detergent aggregates as in LM micelles. Data of TMRM concurs with ANS data in LM micelles. The computed ϕ values using Perrin's equation and the directly measured ϕ values changed in the same direction in buffer and NaCl. These experimental data force one to think in terms of plausible structural perturbations in these polymer assemblies, rather than changes in probe binding per se. Thus, the computed ϕ values indicate that the interpretation of steady state anisotropy values, for these probes, in terms of mobility of probe/probe-domain was reasonable.

The three lifetimes for ANS in BSA, revealed by the time-resolved fluorescence by phase-modulation could arguably reflect the multiple binding sites on BSA, some strong and some relatively weak, owing to the polyelectrolyte nature of the protein and the anionic probe (cf. [15,23,24]). However, laurylmaltoside (LM) micelles, which do not have any charge, showed two lifetimes for ANS. In this context, it is instructive to recall that even for polypeptides with a single tryptophan residue, multiple lifetimes have been reported [21]. Therefore, it may not be an adequate argument to ascribe multiple lifetimes to multiple populations. Rather, it could reveal the microenvironments experienced by the probe [22] (since, in solution, these polymers are in dynamic state) that are collectively reflected in more than one lifetime. Since the bound ANS contributes to the fluorescence intensity signals overwhelmingly, the

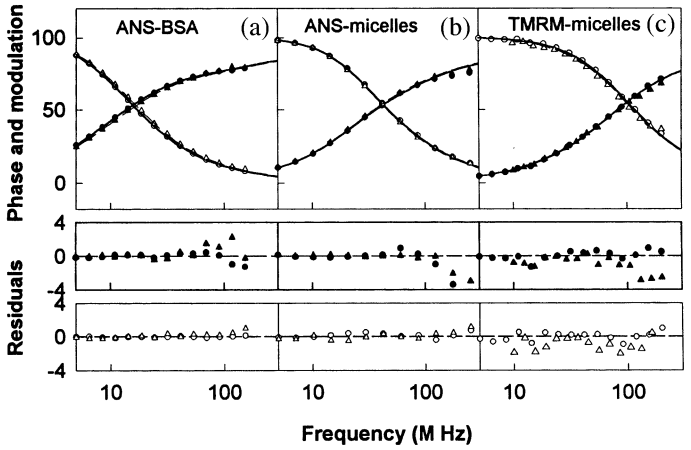

Fig. 7. Frequency-domain data of fluorescence lifetime of ANS and TMRM. Phase angle in degrees (filled symbols) and modulation factor in percentage (open symbols) are plotted in the graphs. (a) Shows data for ANS in BSA in 10 mM sodium phosphate buffer, pH 7.4 (circles) and buffered 1.5 M NaCl (triangles). (b) Shows data for ANS in LM micelles in 10 mM Tris–HCl buffer, pH 7.4 (circles) and buffered 1.5 M NaCl (triangles). (c) Shows data for TMRM in LM micelles in 10 mM Tris–HCl buffer, pH 7.4 (circles) and buffered 1.5 M NaCl (triangles). Residuals after curve fitting are plotted below the respective plots.

steady-state anisotropy computed from steady-state fluorescence intensity signals could adequately reflect the constraint experienced by the probe in its pocket within the protein/polymer assembly. Here in lies the advantage of fluorescence experiments in complex mixtures as opposed to binding studies.

3.6. Plausible role for reciprocal movements

The three polymer systems — proteins, neutral lipid membrane vesicles and non-ionic detergent micelles, all showed reciprocal (opposite) changes in anisotropy of classes of probes typified by ANS and DPH on osmotic perturbations. The conditions for this uniform response varied with the polymer, namely, proteins in electrolyte media, lipid bilayers in non-electrolyte media and LM micelles in both electrolyte and non-electrolyte media.

The thrust of the experimentation was in the evaluation of the conjecture that the biopolymers are uniform in their access to external water and solutes and would respond to dehydration uniformly by compaction (cf. [2,8]). The deployment of highly viscous solutes led to the need to probe the biopolymers with a comparable methodology, which was uniquely offered by fluorescence methodology. The conjecture was confirmed to be valid for DPH class of probes in that high NaCl concentration in the medium led to enhanced anisotropy of DPH. In the case of membrane vesicles these results were comparable to those with anthroyl stearate probes while in BSA, the intrinsic tryptophan showed a comparable response (cf. Fig. 1b). The circular dichroism studies in BSA were also consistent with decreased water potential leading to increased helix rigidity in the interior comparable to the DPH/Trp anisotropy data. The fluorescence lifetime analyses supported a change in the probe rotation.

The anomaly was with ANS class of probes. The cross comparison between different probes using neutral micelles has uniquely excluded ionic effects as causal to this anomalous effect. The decreased anisotropy, consistent with less hindered movement of the probe (fully demonstrated with TMRM) was again consistent with decreased water potential in its milieu. The experiments reported here are consistent with the possibility of surface dehydration leading to enhanced movements in ANS (therefore the exterior region) reciprocal to DPH, which exhibited (corresponding to the interior region) more hindered movement. While dehydration could be the simplest causal agent to suggest, a mechanism for reciprocal movement is conspicuously absent. The results must therefore be considered at an empirical level as a model system to examine the intramolecular movements and hydration within domains. It would be important to examine whether one can account for the 'solute effects' variously described in terms of such movements, which consider the protein surface and bulk measurements of volume, etc. (cf. [1–3,8]). While the nature of coupling within the domains of a polymer and the exterior must find a theoretical solution, at an empirical level, one may begin to ask important questions. One such is the relation between the functionally important movements (FIM) [35] as opposed to equilibrium fluctuations (EF) in catalysis and transport [36]. Here the domains would be the catalytic site and the external thermal sink of the protein.

Acknowledgements

We thank Drs G. Krishnamoorthy, A.D. Gangal and N.V. Joshi for helpful discussions, Dr K.N. Ganesh for the CD spectroscopy facility. This work was supported by grants from the Department of Science and Technology (DST) and The Council of Scientific and Industrial Research (CSIR), India, to V.S. Fellowships from the University Grants Commission, DST and CSIR to C.N.M., Department of Biotechnology and CSIR to Z.E.S., are gratefully acknowledged.

References

[1] V.A. Parsegian, R.P. Rand, N.L. Fuller, D.C. Rau, Osmotic stress for the direct measurement of intermolecular forces, Methods Enzymol. 127 (1986) 400–416.

[2] V.A. Parsegian, R.P. Rand, D.C. Rau, Macromolecules and water: probing with osmotic stress, Methods Enzymol. 259 (1995) 43–94.

[3] S.N. Timasheff, The control of protein stability and association by weak interactions with water: how do solvents affect these processes? Annu. Rev. Biophys. Biomol. Struct. 22 (1993) 67–97.

[4] J.A. Rupley, G. Careri, Protein hydration and function, Adv. Prot. Chem. 41 (1991) 37–172.

[5] A.Yu. Grosberg, A.R. Khokhlov, Giant Molecules, Academic press, New York, 1997.

[6] J.C. Mathai, V. Sitaramam, Stretch sensitivity of transmembrane mobility of hydrogen peroxide through voids in the bilayer, J. Biol. Chem. 269 (1994) 17784–17793.

[7] A. Priev, A. Almagor, S. Yedgar, B. Gavish, Glycerol decreases the volume and compressibility of protein interior, Biochemistry 35 (1996) 2061–2066.

[8] B.S. Kendrick, B.S. Chang, T. Arakawa et al., Preferential exclusion of sucrose from recombinant interleukin-1 receptor antagonist: role in restricted conformational mobility and compaction of native state, Proc. Natl. Acad. Sci. USA 94 (1997) 11917–11922.

[9] B. Honig, A-S. Yang, Free energy balance in protein folding, Advances in Protein Folding, 46, Academic Press, New York, 1995, pp. 27–58.

[10] K.A. Dill, D. Stigter, Modelling protein stability as heteropolymer collapse, Advances in Protein Folding, 46, Academic Press, New York, 1995, pp. 59–104.

[11] J.N. Israelachvili, S. Marcelja, R.G. Horn, Physical principles of membrane organization, Q. Rev. Biophys. 13 (1980) 121–200.

[12] P. Fromherz, Micelle structure: A surfactant block model, Chem. Phys. Lett. 77 (1981) 460–466.

[13] M. Shinitzky, Y. Barenholz, Fluidity parameters of lipid regions determined by fluorescence polarization, Biochim. Biophys. Acta 515 (1978) 367–394.

[14] J. Slavik, Anilinonaphthalene sulfonate as a probe of membrane composition and function, Biochim. Biopys. Acta 694 (1982) 1–25.

[15] D. Matulis, C.G. Baumann, V.A. Bloomfield, R.E. Lovrien, 1-Anilino-8-naphthalene sulfonate as a protein conformational tightening agent, Biopolymers 49 (1999) 451–458.

[16] D. Matulis, R. Lovrien, 1-Anilino-8-naphthalene sulfonate anion-protein binding depends primarily on ion pair formation, Biophys. J. 74 (1998) 422–429.

[17] F. Szoka, D. Papahadjopoulos, Procedure for preparation of liposomes with large internal aqueous space and high capture by reverse-phase evaporation, Proc. Natl. Acad. Sci. USA 75 (1978) 4194–4198.

[18] B. Rubalcava, D.M. Munoz, C. Gitler, Interaction of fluorescent probes with membranes. I. Effect of ions on erythrocyte membranes, Biochemistry 8 (1969) 2742–2747.

[19] A. Cornish-Bowden, R. Eisenthal, Statistical considerations in the estimation of enzyme kinetic parameters by the direct linear plot and other methods, Biochem. J. 139 (1974) 721–730.

[20] P.R. Bevington, Data Reduction and Error Analysis for the Physical Sciences, McGraw-Hill, Inc, New York, 1969.

[21] R. Swaminathan, G. Krishanmoorhy, N. Periasamy, Similarity of fluorescence lifetime distributions for single tryptophan proteins in the random coil state, Biophys. J. 67 (1994) 2013–2023.

[22] J.R. Lakowicz, Principles of Fluorescence Spectroscopy, Plenum Press, New York, 1983.

[23] G. Weber, L.B. Young, Fragmentation of bovine serum albumin by pepsin. I. The origin of the acid expansion of the molecule, J. Biol. Chem. 239 (1964) 1415–1423.

[24] G. Weber, E. Daniel, Cooperative effects in binding by bovine serum albumin. I. The binding of 1-anilino-8-naphthalenesulfonate. Fluorimetric titrations, Biochemistry 5 (1966) 1893–1900.

[25] K. Gekko, Y. Hasegawa, Compressibility–structure relationship of globular proteins, Biochemistry 25 (1986) 6563–6571.

[26] T. Peters, All about Albumin, Academic Press, New York, 1996.

[27] D.L. Veenstra, P.A. Kollman, Modeling protein stability: a theoretical analysis of the stability of T4 lysozyme mutants, Protein Eng. 10 (1997) 789–807.

[28] J.W. Wray, W.A. Baase, J.D. Lindstrom, L.H. Weaver, A.R. Poteete, B.W. Matthews, Structural analysis of a no-contiguous second-site revertant in T4 lysozyme shows that increasing rigidity of a protein can enhance its stability, J. Mol. Biol. 292 (1999) 1111–1120.

[29] D. Cross, L.M. Loew, Fluorescent indicators of membrane potential: microspectrofluorometry and imaging, in: D.L. Taylor, Yu-Li. Wang (Eds.), Fluorescence Microscopy of Living Cells in Culture. Part B. Quantitative Fluorescence Microscopy-Imaging and Spectroscopy. Methods in Cell Biology, 30, Academic Press, San Diego, USA, 1989, pp. 193–218.

[30] A.G. Lee, Functional properties of biological membranes: A physical chemical approach, Progr. Biophys. Molec. Biol. 29 (1975) 1–56.

[31] D.W.R. Gruen, A model for the chains in amphiphilic aggregates. 1. Comparison with a molecular dynamics simulation of a bilayer, J. Phys. Chem. 89 (1985) 146–153.

[32] D.W.R. Gruen, A model for the chains in amphiphilic aggregates. 2. Thermodynamic and experimental comparison for aggregates of different shape and size, J. Phys. Chem. 89 (1985) 153–163.

[33] M. Straume, B.J. Litman, Equilibrium and dynamic structure of large, unilamellar, unsaturated acyl chain phosphatidylcholine vesicles. Higher order analysis of 1,6-diphenyl-1,3,5-hexatriene and 1-[4-(trimethylammonio)phenyl]-6-phenyl-1,3,5-hexatriene anisotropy decay, Biochemistry 26 (1987) 5113–5120.

[34] M. Straume, B.J. Litman, Influence of cholesterol on equilibrium and dynamic bilayer structure of unsaturated acyl chain phosphatidylcholine vesicles as determined from higher order analysis of fluorescence anisotropy decay, Biochemistry 26 (1987) 5121–5126.

[35] H. Frauenfelder, E. Gratton, Protein dynamics and hydration, Methods Enzymol. 127 (1986) 207–216.

[36] G.R. Welch, B. Somogyi, S. Damjanovich, The role of protein fluctuations in enzyme action: a review, Progr. Biophys. Molec. Biol. 39 (1982) 109–146.